Theor Chem Acc (2000) 104:123–130
DOI 10.1007/s002140000117

Theoretical
Chemistry Accounts

Regular article

A genetic algorithm for the structural optimization of Morse clusters

Chris Roberts, Roy L. Johnston, Nicholas T. Wilson

School of Chemistry, University of Birmingham, Edgbaston, Birmingham B15 2TT, UK

Received: 27 October 1999 / Accepted: 7 December 1999 / Published online: 19 April 2000

Abstract. This article describes the application of a genetic algorithm for the structural optimization of 19–50-atom clusters bound by medium-range and short-range Morse pair potentials. The GA is found to be efficient and reliable for finding the geometries corresponding to the previously published global minima [Doye JPK, Wales DJ (1997) *J Chem Soc Faraday Trans* 93: 4233]. Using the genetic algorithm, only a relatively small number of energy evaluations and minimizations are required to find the global minima. By contrast, a simple random search algorithm often cannot find the global minima of the larger clusters, even after many thousands of searches.

Key words: Genetic algorithms – Clusters – Morse potential – Global minimization

1 Introduction

The genetic algorithm (GA) [1–3] is a search technique based on the principles of natural evolution. It uses operators that are analogues of the evolutionary processes of genetic crossover, mutation and natural selection to explore multidimensional parameter spaces. A GA can be applied to any problem where the variables to be optimized (genes) can be encoded to form a string (chromosome). Each string represents a trial solution of the problem. The GA operators exchange information between the strings to evolve new and better solutions. A crucial feature of the GA approach is that it operates effectively in a parallel manner: many different regions of parameter space are investigated simultaneously. Furthermore, information concerning different regions of parameter space is passed actively between the individual strings by the crossover procedure, thereby disseminating genetic information throughout the population. The GA is an intelligent search mechanism that is able to learn which regions of the search space represent good solutions, via the concept of schemata [1].

Whether one is using empirical atomistic potentials or ab initio molecular orbital or density functional theory to describe the bonding in clusters, one of the objectives is to find, for a given cluster size, the arrangement of atoms (or ions or molecules) corresponding to the lowest potential energy, i.e. the global minimum on the potential-energy hypersurface. However, as the number of minima rises extremely rapidly with increasing cluster size, finding the global minimum is a nontrivial (in fact NP-hard!) problem. Traditional Monte Carlo and molecular dynamics simulated annealing approaches often encounter difficulties finding global minima for particular types of interatomic interactions (such as, for example, the short-range Morse potential discussed later) [4]. It is for this reason that GAs have found increasing use in the area of finding global minima for clusters, i.e. for cluster geometry optimization.

The use of GAs for optimizing cluster geometries was pioneered by Hartke (for small silicon clusters) [5] and Xiao and Williams (for molecular clusters) [6]. In both cases the cluster geometries were binary encoded, with the genetic operators acting in a bitwise fashion on the binary strings. Hartke and coworkers have subsequently published the results of GA geometry optimizations for a number of different types of cluster [7–10].

An important stage in the evolution of GAs for cluster optimization occurred when Zeiri [11–13] introduced a GA that operated on the real-valued Cartesian coordinates of the clusters. This approach allowed the cluster to be represented in terms of continuous variables and removed the requirement for encoding and decoding binary genes.

The next significant step in the development of GAs for cluster optimization was due to Deaven and coworkers [14, 15], who performed a gradient-driven local minimization of the cluster energy after each new cluster was generated. As Doye and Wales [16] have pointed out, the introduction of local minimization effectively transforms the cluster potential-energy hypersurface into a stepped surface, where each step corresponds to a basin of attraction of a local minimum on the potential-

Correspondence to: R. L. Johnston
e-mail: roy@tc.bham.ac.uk

energy surface. This simplification of the surface greatly facilitates the search for the global minimum by reducing the space that the GA has to search. This same principle underpins the basin hopping Monte Carlo method developed by Doye and Wales [16] and the "Monte Carlo plus energy minimization" approach of Li and Scheraga [17]. These related methods have proved very efficient for the structural optimization of clusters, crystals and biomolecules [18]. In the GA context, such local minimization corresponds to Lamarckian, rather than Darwinian evolution, as individuals pass on a proportion of the characteristics that they have acquired to their offspring. In the case of clusters, these acquired characteristics are the geometries after local minimization, rather than the characteristics they themselves inherited.

Another significant development in cluster optimization GAs, also due to Deaven and coworkers [14, 15], was the introduction of the three-dimensional "cut and splice" crossover operator. This operator, which has been employed in most subsequent cluster GA work, gives a more physical meaning to the crossover process. In this crossover mechanism, good schemata correspond to regions of the parent clusters which have low-energy local structure.

Recent work on cluster geometry optimization using GAs, for a variety of potentials and types of cluster, has been reported by Neisse and coworkers [19–22], Pullan [23–25], Hobday and Smith [26], Curotto et al. [27], Wolf and Landman [28] and Chaudhury and Bhattacharyya [29]. Michaelian, Garzón and coworkers [30–33] have developed a "symbiotic algorithm", based on GA principles, and applied it to metal clusters bound by many-body potentials. An up-to-date database of the application of GAs (and other evolutionary algorithms) to clusters (and other optimization problems) is maintained by Clark [34].

To our knowledge, GAs have not previously been employed to optimize clusters with potential-energy surfaces described by the Morse potential. Doye and Wales [4] have described the structural consequences of varying the range of the Morse potential. Using the basin hopping Monte Carlo approach [16], they found global minima for Morse clusters with different range parameters and noted that the short-range Morse potential (which has many local minima and a very "noisy" potential-energy surface) presents a particular challenge for global optimization techniques [4]. Their results (cluster coordinates and energies) are available on the Cambridge Cluster Database Web site [35]. We, therefore, decided to write and apply a GA to find global minima for Morse clusters, especially in the challenging case of short-range Morse potentials. Preliminary results for small clusters ($N < 10$) using a medium-range Morse potential (together with many-body potentials for carbon and aluminium clusters) have previously been reported [36].

2 Methodology

2.1 The Morse potential

The Morse potential is a pairwise additive potential [37], which depends only on the separations, r_{ij}, between pairs of atoms:

$$V_{ij}^{\mathrm{M}} = D_{\mathrm{e}}[\mathrm{e}^{\alpha(1-r_{ij}/r_{\mathrm{e}})}(\mathrm{e}^{\alpha(1-r_{ij}/r_{\mathrm{e}})} - 2)] \ , \tag{1}$$

where D_{e} is the bond dissociation energy (assumed constant for all interactions in a homonuclear cluster), r_{e} is the equilibrium bond length and α is the range exponent of the potential. Short-range Morse potentials correspond to high values of α.

The potential used here, as in the work of Doye and Wales [4], is a simplified, scaled version of the Morse potential with D_{e} and r_{e} both set to 1

$$V_{ij}^{\mathrm{M}} = \mathrm{e}^{\alpha(1-r_{ij})}(\mathrm{e}^{\alpha(1-r_{ij})} - 2) \ . \tag{2}$$

This provides a non-atom-specific potential which depends on a single parameter: the range exponent, α. In this study, we compare short-range ($\alpha = 14$) and medium-range ($\alpha = 6$) Morse potentials.

The total potential energy of a cluster of N atoms is obtained by summing over all atom pairs:

$$V_{\mathrm{clus}} = \sum_{i}^{N-1} \sum_{j>i}^{N} V_{ij}^{\mathrm{M}} \ . \tag{3}$$

It should be noted that, as all V_{clus} values are negative, the expression "low energy" actually refers to high values of $-V_{\mathrm{clus}}$.

2.2 The GA

A flow chart representing the operation of our cluster geometry optimization GA program [38] is shown in Fig. 1 and the basic features of the GA are described in the following sections.

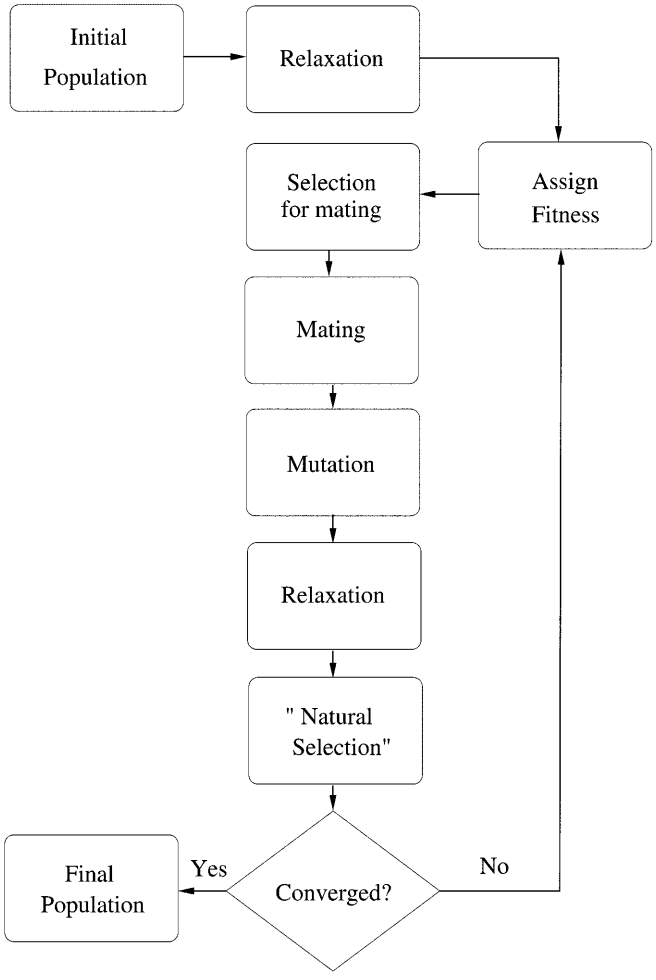

Fig. 1. Schematic flow chart for the cluster geometry optimization GA program

2.2.1 Generation of the initial population

For a given cluster nuclearity (N), a number of clusters, N_{pop}, (typically ranging from 10 to 30) are generated at random to form the initial population (the "zeroth generation"). We have followed the approach of Zeiri [11–13] in using the real-valued Cartesian coordinates of the cluster atoms as the genes. The x, y and z coordinates are chosen randomly in the range $[0, N^{1/3}]$ [39]. This ensures that the cluster volume scales correctly with cluster size, i.e. linearly with N. All the clusters in the initial population are then relaxed into the nearest local minima, by minimizing the cluster potential energy as a function of the cluster coordinates, using the quasi-Newton (L-BFGS) routine [40, 41]. This routine utilizes analytical first derivatives of the potential.

The GA operators of mating (crossover), mutation and selection (on the basis of fitness) are performed to evolve one generation into the next. In this work, we use the term "mating" to refer to the process by which two parent clusters are combined to generate offspring. The mechanism, at the chromosome level, by which genetic material is combined, is termed "crossover".

2.2.2 Fitness

Each cluster is assigned a fitness value based on its total potential energy (V_{clus}), such that low-energy clusters (high $-V_{clus}$) have high fitness and high-energy clusters (low $-V_{clus}$) have low fitness. We have adopted dynamic fitness scaling so that, in each generation, the fittest (lowest energy) cluster has a fitness of 1. We have found that the most suitable fitness function, i.e. that leading to the most efficient GA, has an exponential form. The fitness (F_i) of the ith member of the population (with $V_{clus} = V_i$) is given by

$$F_i = \exp\left(-\rho\left[\frac{V_i - V_{min}}{V_{max} - V_{min}}\right]\right) , \quad (4)$$

where V_{max} and V_{min} are the V_{clus} values of the highest and lowest energy clusters in the current population and ρ is a scaling factor (typically set to 3).

The fitness of the best (lowest energy) member of the population (with $V_i = V_{min}$) is 1, while the fitness of the worst (with $V_i = V_{max}$) is $e^{-\rho}$.

2.2.3 Selection of parents for mating

The selection of parents for mating is accomplished using a variant of the roulette wheel method [2]. A cluster is picked at random and is accepted for mating if its fitness value is greater than a randomly generated number between 0 and 1, i.e. if $F_i > R[0, 1]$. If the candidate cluster is rejected for mating, then another is picked and the process is repeated. In this way, low-energy clusters (with high fitness values) are more likely to be selected for mating and therefore to pass on their structural characteristics into the next generation. (Each cluster may be chosen more than once for mating but self-mating is not allowed.) Once a pair of parents has been selected, the parents are subjected to the mating operation.

2.2.4 Mating/crossover

Mating is carried out using a variant of the cut and splice crossover operator of Deaven and coworkers [14, 15]. In the original work of Deaven and Ho, a plane, passing through the centre of mass of each cluster was chosen. The clusters were then cut about this plane and complementary halves were spliced together in order to generate the offspring or child clusters. In our implementation of the cut-and-splice operation, as shown schematically in Fig. 2, random rotations (about two perpendicular axes) are performed on both parent clusters and then both clusters are cut horizontally – parallel to the xy plane – at a random point and complementary fragments are spliced together. In practice, this is accomplished by ranking the coordinates of the component atoms of each rotated cluster in order of decreasing z coordinate and then selecting the first (highest z) $N - M$ coordinates from the first parent and the last (lowest z) M coordinates from the second parent and combining them to generate a child cluster with N atoms. The choice of a random crossover point, which reduces to the selection of a random integer M in the range $[1, N - 1]$, leads to a greater number of possible offspring from a given pair of parents, thereby helping to maintain population diversity. Though we have chosen only to generate one child from each mating operation, the creation of two children may be desirable in cases where mating leads to too few children of comparable fitness to their parents.

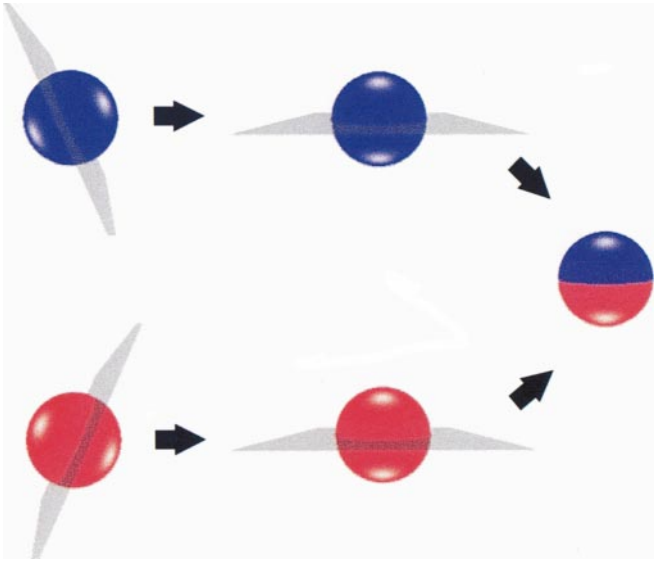

Fig. 2. The mating procedure

Mating continues until a predetermined number of matings (N_{mat}) have occurred. This corresponds to the generation of N_{mat} children. The number of matings is generally set to approximately 80% of the population size, i.e. $N_{mat} = \text{int}(0.8\, N_{pop})$. Unless selected for mutation (see later), the child clusters are subsequently relaxed into the nearest local minima, as described previously. The local minimization step, obviously changes the structure of the child cluster, and this structural rearrangement will be greatest in the region of the join between the two fragments donated by its parents. As the clusters get larger, however, the perturbation due to the local minimization should become relatively smaller and confined to the join region. In this way, the principle of schemata (where fragments with low-energy arrangements of atoms are more likely to be passed on) should apply.

2.2.5 Mutation

While the mating/crossover operation leads to a mixing of genetic material in the offspring, with the exception of the small perturbation in the join region, no new genetic material is introduced. For small populations, this can lead to population stagnation and premature convergence on a nonoptimal structure. In an attempt to avoid stagnation and to maintain population diversity, a mutation operator is introduced.

In our GA, mutation is performed on the set of N_{mat} offspring, with each child cluster having the same probability (P_{mut}) of being mutated. Thus, in each cycle, the number of mutants created is approximately $P_{mut}N_{mat}$. Mutation is achieved by assigning new random coordinates (again in the range $[0, N^{1/3}]$) to approximately one-third of the atoms in the cluster.

Mutant clusters are subsequently relaxed into the nearest local minima, as described previously.

2.2.6 "Natural selection"

We have adopted a steady-state GA, i.e. one that employs a constant population size, so the next stage of the GA is to select N_{pop} clusters to form the next generation. The set of N_{pop} "old" clusters (from the previous generation) and the N_{mat} "new" clusters (children and mutants) are ranked in order of potential energy. The top N_{pop} clusters, i.e. those with lowest energy and, therefore, highest

fitness, are then selected to constitute the population in the next generation.

This selection process, which is the analogue of natural selection in biological evolution, is performed on the basis of fitness – survival of the fittest! Since fitness is directly related to potential energy, through Eq. (3), however, it is not actually necessary to calculate fitnesses prior to selection.

Our GA can be described as "elitist", since a minimum of 20% ($N_{pop} - N_{mat}$, with $N_{mat} = 0.8\,N_{pop}$) of the lowest energy clusters from the previous generation are carried forward to the next generation. Elitism ensures that the lowest energy cluster found during the run of the GA will not be lost, in other words the best member of the population cannot get worse.

2.2.7 Subsequent generations

Once the new generation has been formed, the potential energies of the best (V_{min}) and worst (V_{max}) members of the population are recorded and the fitness values calculated for the entire population. The whole process of mating, mutation and selection is then repeated for a specified number (N_{gen}) of generations or until the population converges (i.e. all clusters are identical) – ideally on the structure corresponding to the global minimum. Because of the stochastic nature of the GA, the GA program is run several times for each cluster nuclearity.

2.2.8 Values of GA parameters

Our cluster-geometry-optimization GA program [38] was used to study Morse clusters ($\alpha = 6$ and 14) with $N = 19$–50. Preliminary calculations were performed on a number of trial clusters and the following optimum values were obtained for the GA program parameters: $N_{pop} = 10$; $N_{mat} = 8$; $P_{mut} = 0.1$; and $N_{gen} = 10$–300 (increasing with cluster size).

2.3 Random search

A random search (RS) algorithm was also used to illustrate the problem in locating global minima for even quite simple pair potentials and to demonstrate the efficiency of the GA for finding the global minima. The RS algorithm, which has been discussed in detail elsewhere [42], generates a large number of clusters randomly, as described previously, and relaxes them, using the L-BFGS routine, into the nearest minimum.

3 Results and discussion

3.1 Comparison of GA and RS methods

The efficiency of the GA was compared with the RS algorithm by performing five different runs of the GA and the RS algorithm for each of five cluster sizes (N) and a Morse exponent (α) of 6. Different random number seeds were used in the five runs so as to generate distinct initial populations for the GA program and a different set of random starting geometries for the RS algorithm.

The success or failure of the RS algorithm in finding the previously published [4] global minima is summarized in Table 1. N_{search} is the number of random searches performed in each run of the RS program, i.e. the number of starting geometries which are minimized using the L-BFGS routine. The table shows that the RS algorithm was only able to find the lowest energy structure for the two smallest cluster sizes. Since the number of minima rises exponentially with increasing cluster size [18], even doubling or quadrupling the number of searches fails to find the global minima for $N = 40$ and 50. In the case of the 50-atom cluster, minimizing 10000 random cluster geometries (five runs of 2000 searches each) failed to locate the global minimum! This problem will be even worse for the short-range ($\alpha = 14$) Morse potential, which has a greater number of local minima [4].

Table 1. Indication of the success or failure of the random search (*RS*) algorithm to find the reported global minima for five runs of the RS routine at each of five cluster nuclearities (N) for $\alpha = 6$. N_{search} is the number of searches performed in each run of the RS algorithm

N	N_{search}	Global minimum found?				
		Run 1	Run 2	Run 3	Run 4	Run 5
20	50	No	No	Yes	Yes	Yes
30	500	No	Yes	No	No	No
40	1000	No	No	No	No	No
50	2000	No	No	No	No	No

The number of calls (N_{min}) made to the L-BFGS local minimization routine (until the previously published [4] global minimum was found) for each of the separate runs of the GA are listed in Table 2. Ranges are given for N_{min} because it is only known in which generation the global minimum was found and $0.8 \times N_{pop}$ new clusters (children and mutants) are generated (and minimized) in each generation. The average range is also given for each of the five nuclearities. These results demonstrate that the GA was able to locate the global minimum in each of the runs, for all cluster sizes. As expected, the average number of minimizations increases with increasing cluster size, reflecting the increase in the number of local minima. This trend explains why, for larger clusters, we increase the number of generations (N_{gen}) for which the GA is run. The success of the GA compared with the RS algorithm is undeniable. We are currently working on a detailed comparison of the efficiency and reliability of our GA relative to other global optimization techniques, such as Monte Carlo, molecular dynamics simulated annealing and Monte Carlo basin hopping.

3.2 GA optimization of 19–50-atom Morse clusters

Our GA has located all the previously published global minima [4] for Morse clusters with 19–50 atoms, both for medium-range ($\alpha = 6$) and short-range ($\alpha = 14$) Morse potentials. As we did not find any lower energy structures in this size regime, our results support the global minima assigned by Doye and Wales on the basis of their basin hopping Monte Carlo optimizations [4]. The potential energies (V_{clus}) of the global minima are listed in Table 3. The fact that the global minima for $\alpha = 14$ have higher (less negative) energies than those for $\alpha = 6$ is because the short range of the potential results in the stabilizing contributions from remote atoms being relatively unimportant. This also explains why the difference in V_{clus} increases with N. The difference scales almost linearly with size, as evidenced by the fact that the difference in average binding energies,

$$\Delta E_b = E_b(\alpha = 6) - E_b(\alpha = 14)\ , \qquad (5)$$

Table 2. The number of local minimization steps (N_{min}) required by the genetic algorithm (*GA*) to find the reported global minimum energy structures for five GA runs at each of five cluster nuclearities (N) for $\alpha = 6$. N_{pop} is the population size for each of the runs

N	N_{pop}	N_{min}					
		Run 1	Run 2	Run 3	Run 4	Run 5	Average
20	10	11–16	≤10	≤10	35–42	11–16	19–24
30	10	27–34	131–138	267–274	163–170	67–74	131–138
40	10	275–282	171–178	59–66	75–82	427–434	203–210
50	10	227–234	235–242	707–714	315–322	451–458	395–402

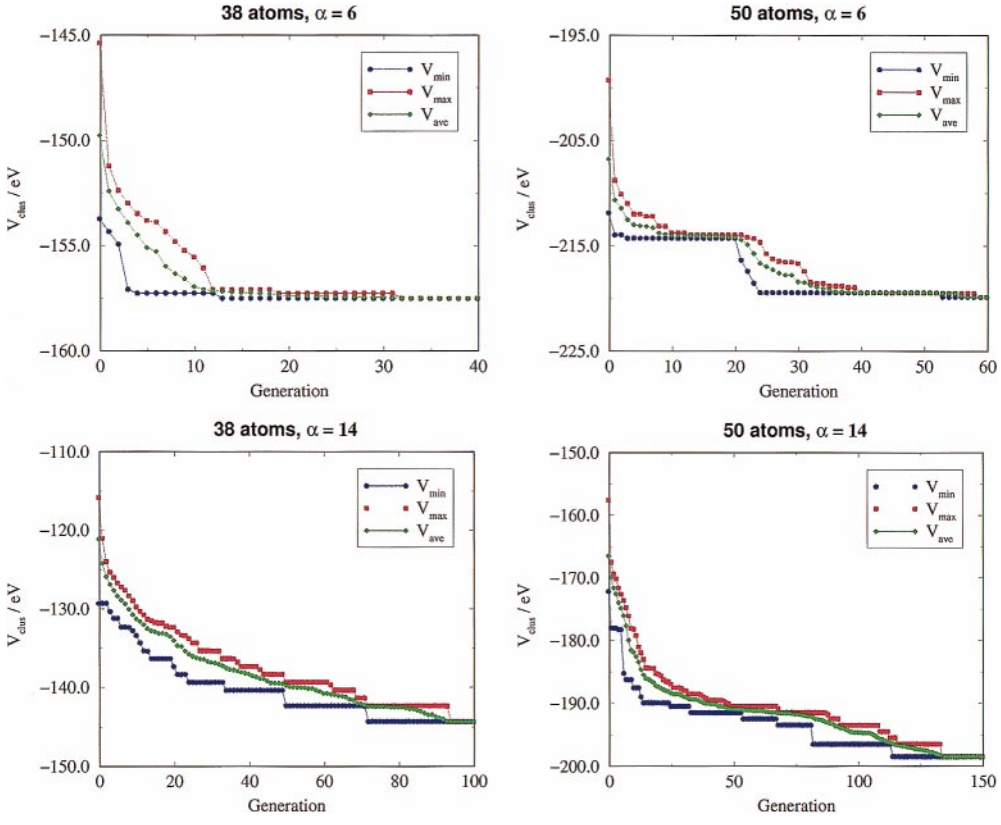

Fig. 3. Evolutionary Progress Plots [43] for 38 and 50 atom Morse clusters with $\alpha = 6$ and $\alpha = 14$

with

$$E_b = \frac{-V_{clus}}{N} \quad , \tag{6}$$

is approximately independent (about 0.4) of cluster size.

The structures of the global minima for $\alpha = 6$ and 14 are shown in Table 4. These structures have been discussed in detail by Doye and Wales [4], the most obvious difference between the two potentials being that the longer-range ($\alpha = 6$) potential tends to favour polytetrahedral, icosahedral geometries, while the short-range ($\alpha = 14$) potential favours decahedral and face-centred-cubic-like packing (such as the truncated octahedral cluster which is the global minimum for $N = 38$).

3.3 Cluster evolution

Evolutionary progress plots (EPPs [43]) of energy (V_{min}, V_{max} and V_{ave} – the average value of V_{clus} for the population) as a function of generation are shown in Fig. 3 for two cluster sizes ($N = 38$ and 50) for both $\alpha = 6$ and 14.

Table 3. Energies (V_{clus}/eV) of global minima found for Morse clusters with N = 19–50 atoms for α = 6 and 14

N	α = 6	α = 14	N	α = 6	α = 14
19	−68.492285	−60.812425	35	−141.957188	−129.737360
20	−72.507782	−64.791953	36	−147.381965	−133.744666
21	−76.529139	−68.783571	37	−151.891203	−138.708582
22	−81.136735	−72.791747	38	−157.477108	−144.321054
23	−86.735494	−77.302495	39	−163.481990	−148.327400
24	−90.685398	−81.309508	40	−167.993097	−152.333745
25	−95.127899	−85.477376	41	−172.526828	−156.633479
26	−100.549598	−90.210764	42	−177.680221	−160.641020
27	−104.745275	−94.219798	43	−183.092699	−165.634973
28	−108.997831	−98.331711	44	−187.626292	−169.642441
29	−114.145949	−102.774589	45	−192.954739	−174.511632
30	−118.432844	−106.765372	46	−199.177751	−178.519320
31	−122.857743	−111.760670	47	−203.704178	−183.508227
32	−127.771395	−115.767561	48	−209.044000	−188.888965
33	−132.287430	−120.741345	49	−215.253702	−192.898412
34	−136.797544	−124.748271	50	−219.820229	−198.455632

In all cases there is a rapid improvement in the population (a sharp drop in V_{min}, V_{max} and V_{ave}) in the early generations relative to the initial, randomly

generated population (“generation 0”). This early improvement is due entirely to the mating process. Subsequent, less dramatic improvement occurs in a stepwise fashion and may be due to mating or mutation.

Figure 3 shows that, in all four cases, the population converges on a single structure – as evidenced by V_{min}, V_{max} and V_{ave} becoming equal. The converged structure was found to be the global minimum in each case. The face-centred-cubic-like truncated octahedral geometry of the 38-atom ($\alpha = 14$) Morse cluster is difficult to find with most global optimization techniques [4], but is here found before the 100th generation – even for a small population size of 10. Comparing EPPs for $N = 38$ and $N = 50$ confirms that the GA must, in general, be run for a greater number of generations for larger cluster sizes. Similarly, comparison of the EPPs for $\alpha = 14$ with those for $\alpha = 6$ confirms that the short-range Morse potential is more difficult to search [4], taking 2–3 times as many generations to find the global minima.

Table 4. Global minima for Morse clusters with $N = 19$–50 atoms for $\alpha = 6$ and $\alpha = 14$

N	$\alpha = 6$	$\alpha = 14$
19		
20		
21		
22		
23		
24		
25		

4 Conclusions

We have shown that the GA described here is both efficient and reliable for finding the geometries

Table 4. (Contd.)

N	$\alpha = 6$	$\alpha = 14$
26		
27		
28		
29		
30		
31		
32		
33		
34		

Table 4. (Contd.)

N	$\alpha = 6$	$\alpha = 14$
35		
36	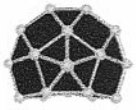	
37		
38		
39		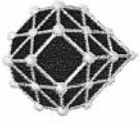
40		
41		
42		

Table 4. (Contd.)

N	$\alpha = 6$	$\alpha = 14$
43		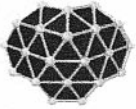
44		
45		
46	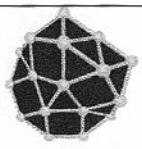	
47		
48		
49		
50		

corresponding to the previously published global minima for Morse clusters with between 19 and 50 atoms – both for medium-range ($\alpha = 6$) and for the more challenging short-range ($\alpha = 14$) Morse potentials. A relatively small number (of the order of tens or hundreds) of energy evaluations and minimizations are required before the global minima are found. A comparison has been made with a simple RS algorithm, which often cannot find the global minima for the larger clusters even after performing many thousands of minimizations.

One of the reasons for choosing Morse clusters for this study was that a large database of structures and energies already existed [4, 35], which meant that we could test the efficiency and reliability of our GA program for cluster geometry optimization. Our GA has been applied to a wide range of clusters bound by pair and many-body potentials, for which the global minima were not previously known (or predicted) [36]. Further studies are currently being carried out to compare our GA with other techniques for global optimization of cluster geometries for a variety of cluster types.

The structures and coordinates of the global minima reported here can be found on the Birmingham Cluster Web site [44].

Acknowledgements. The authors wish to thank F. R. Manby for many helpful discussions. C.R. and N.T.W. are grateful to the EPSRC for PhD studentships and R.L.J. acknowledges financial support from the Royal Society (RSRG/16180) and the University of Birmingham.

References

1. Holland J (1975) Adaptation in natural and artificial systems. University of Michigan Press, Ann Arbor
2. Goldberg DE (1989) Genetic algorithms in search, optimization and machine learning. Addison-Wesley, Reading, Mass
3. Cartwright HM (1993) Applications of artificial intelligence in chemistry. Oxford University Press, Oxford
4. Doye JPK, Wales DJ (1997) J Chem Soc Faraday Trans 93: 4233
5. Hartke B (1993) J Phys Chem 97: 9973
6. Xiao Y, Williams DE (1993) Chem Phys Lett 215: 17
7. Hartke B (1995) Chem Phys Lett 240: 560
8. Hartke B (1996) Chem Phys Lett 258: 144
9. Gregurick SK, Alexander MH, Hartke B (1996) J Chem Phys 104: 2684
10. Hartke B, Schutz M, Werner HJ (1998) Chem Phys 239: 561
11. Zeiri Y (1995) Phys Rev E 51: 2769
12. Zeiri Y (1997) Comput Phys Commun 103: 28
13. Zeiri Y (1998) J Phys Chem A 102: 2785
14. Deaven DM, Ho KM (1995) Phys Rev Lett 75: 288
15. Deaven DM, Tit N, Morris JR, Ho KM (1996) Chem Phys Lett 256: 195
16. Doye JPK, Wales DJ (1997) J Phys Chem A 101: 5111
17. Li Z, Scheraga HA (1998) J Mol Struct (THEOCHEM) 179: 333
18. Wales DJ, Scheraga HA (1999) Science 285: 1368
19. Niesse JA, Mayne HR (1996) Chem Phys Lett 261: 576
20. Niesse JA, Mayne HR (1996) J Chem Phys 105: 4700
21. Niesse JA, Mayne HR (1997) J Comput Chem 18: 1233
22. White RP, Niesse JA, Mayne HR (1998) J Chem Phys 108: 2208
23. Pullan WJ (1997) Comput Phys Commun 107: 137
24. Pullan WJ (1997) J Chem Inf Comput Sci 37: 1189
25. Pullan WJ (1997) J Comput Chem 18: 1096
26. Hobday S, Smith R (1997) J Chem Soc Faraday Trans 93: 3919
27. Curotto E, Matro A, Freeman DL, Doll JD (1998) J Chem Phys 108: 729
28. Wolf MD, Landman U (1998) J Phys Chem A 102: 6129
29. Chaudhury P, Bhattacharyya S (1999) Chem Phys 241: 313
30. Michaelian K (1998) Chem Phys Lett 293: 202
31. Garzón KMIL, Beltrán MR, Posada-Amarillas A, Ordejón P, Artacho E, Sánchez-Portal D, Soler JM (1998) Phys Rev Lett 81: 1600
32. Michaelian K (1998) Am J Phys 66: 231
33. Michaelian K, Rendon N, Garzón IL (1999) Phys Rev B 60: 2000
34. Clark DE (1999) Evolutionary algorithms in computer-aided molecular design. http://panizzi.shef.ac.uk/cisrg/links/ea_-bib.html
35. Wales DJ, Doye JPK, Dullweber A, Naumkin FY (1997) The Cambridge Cluster Database. http://brian.ch.cam.ac.uk/CCD.html
36. Manby FR, Johnston RL, Roberts C (1998) Commun Math Comput Chem 38: 111
37. Morse PM (1929) Phys Rev 34: 57
38. Johnston RL, Roberts C (1999) Cluster geometry optimization genetic algorithm program. University of Birmingham
39. Press WH, Teukolsky SA, Vetterling WT, Flannery BP (1992) Numerical recipes in Fortran 77 2nd edn. Cambridge University Press, Cambridge
40. Byrd RH, Lu P, Nocedal J, Zhu C (1995) J Sci Comput 16: 1190
41. Zhu C, Byrd RH, Lu P, Nocedal J (1995) Northwestern University EECS Technical Report NAM12
42. Lloyd LD, Johnston RL (1998) Chem Phys 236: 107
43. Harris KDM, Johnston RL, Kariuki BM (1998) Acta Cryst A 54: 632
44. Johnston RL, Wilson NT (1999) Birmingham Cluster Web site. http://www.tc.bham.ac.uk/bcweb